Materials Science Forum Vols 312-314 (1999) pp 43-48

doi:10.4028/www.scientific.net/MSF.312-314.43

Mechanically-Driven Solid State Amorphization and Nanocrystallization in Selenium

K. Lu, F.Q. Guo, Y.H. Zhao and Z.H. Jin

State Key Laboratory for Rapidly Solidified Non-Equilibrium Alloys (RSA), Institute of Metal Research, Chinese Academy of Sciences, Shenyang 110015, China

Keywords: Mechanical Attrition, Ball-Milling, Solid State Amorphization, Nanocrystallization, Selenium, Molecular Structure

Abstract. An amorphous-nanocrystalline-amorphous phase transformation was observed in element selenium when a melt-quenched amorphous Se (a-Se) was subjected to ball-milling. The mechanical attrition (MA) induced nanocrystallization process of a-Se and the solid state amorphization of nanocrystalline Se were experimentally investigated by using quantitative XRD, DSC, TEM, XPS, infrared and Raman spectroscopy. An evident molecular structure difference was detected between the as-milled and the as-quenched a-Se samples, while no detectable difference in electronic properties were observed among different states of the Se samples. The underlying mechanism for the solid state amorphization in the element was discussed with respect to the microstructure information of the nanocrystalline phases during ball milling.

Introduction

Phase equilibrium between amorphous solids and nanocrystalline states under different circumstances (such as annealing, plastic deformation, pressure, etc.) has drawn increasing attention owing to the need for a fundamental understanding of the nature of these metastable solid states and the interests in developing advanced materials with high performance [1,2]. Among various processing techniques, mechanical attrition (MA) provides an effective approach to induce phase transformation between these metastable structures. The MA (as performed normally by ball milling) is considered to be a process consisting of fracture and cold-welding of the milled material. In many systems, solid state amorphization has been realized completely (such as in some alloys and intermetallics [3,4]) or partially (Si and Ge [5,6]) by MA. The MA-induced amorphization is attributed to the accumulation of defects (such as lattice defects and grain boundaries) that raise the free energy of the defective nanocrystalline phase above that of the amorphous phase. Meanwhile, MA-induced nanocrystallization of amorphous alloys was observed recently in Fe- and Al-based glasses [7,8]. It means both the solid-state amorphization (of nanocrystalline phases) and nanocrystallization (of amorphous phases) can be realized via MA. These two processes, with fundamentally different mechanisms, are opposite in direction from a thermodynamic point of view. It therefore seems of interest to carry out an intensive study on MA-induced phase transformations between the amorphous and nanocrystalline states in a simple elemental system.

In this paper, we reported an experimental investigation on the metastable phase transformation in Se subjected to ball-milling. A nanocrystallization of amorphous Se as well as a mechanically-driven solid state amorphization of nanocrystalline Se were observed [9]. The microstructure evolution and its intrinsic mechanism in the metastable element will be explored by means of quantitative structure and thermal analyses.

Experimental

Pure (99.999 at.%) amorphous elemental Se was prepared by means of the melt quenching technique, which was used as the starting material for ball milling. The amorphous nature of the as-quenched Se was verified using x-ray diffraction (XRD), transmission electron microscopy (TEM),

and differential scanning calorimeter (DSC) techniques. The ball milling was performed in a high-energy vibrating ball mill (Super-Misuni, Nisshin-Giken) under a flowing argon atmosphere. The milling vial was kept cool at 0 °C. The ball-to-sample weight ratio was 8:1. Structural characterization was made using a Rigaku x-ray diffractometer with Cu Kα radiation and a Philips EM420 transmission electron microscope with an accelerating voltage of 120 kV. Characterization of the molecular structure was carried out by means of infrared (IR) and Raman spectroscopy (RS) techniques. RS measurements were performed on a Nicolet 910 FT-Raman spectrometer equipped with a Nd:YOV_4 solid laser source (the wavelength of the laser is 1064 nm). The Raman spectra were recorded at a resolution of 4 cm^{-1} with 200 scans per spectrum in the range of 100 - 600 cm^{-1}. IR measurements were made using a Nicolet Magna FTIR-750 II spectrometer equipped with a diffuse reflection accessory. The IR spectra were recorded at a resolution of 8 cm^{-1} with 128 scans per spectrum in the range of 100 - 400 cm^{-1}. Thermal analysis was carried out with a differential scanning calorimeter (DSC-7, Perkin-Elmer). Aluminum pans were used for both the sample holder and the reference. The temperature (with an accuracy of ± 0.02 K) and energy (± 0.04 mJ/s) measurements were calibrated by means of standard In and Zn samples. Chemical analysis and energy-dispersive x-ray analysis showed that in the sample milled for 300 min, oxygen content is less than 0.1 wt.% and Fe contamination is below 0.02 wt.%.

Results and Discussion

Amorphous-nanocrystalline-amorphous transition. Figure 1 presents the XRD patterns for the as-quenched Se samples milled for different periods of time (t_m). During the initial stage of milling, the as-quenched a-Se gradually crystallizes, showing traces of diffraction lines of trigonal Se (t-Se) besides the two typical diffuse peaks for a-Se. With increasing t_m, the t-Se lines increase in their intensities while the peaks for the a-Se diminish. When $t_m \geq 30$ min, only t-Se can be found in the XRD pattern. From the XRD line broadening, we estimated the mean grain size of the as-crystallized t-Se, as about 13 nm, which coincides with estimates (~ 15 nm) from the TEM observations. Dark-field TEM images and the corresponding electron diffraction patterns indicated that the sample milled for 30 min consisted of fine equiaxial grains with random crystallographic orientations. Their microstructure characteristics are rather similar to the thermal crystallization products [10].

Further milling of the as-crystallized nanocrystalline t-Se leads to a decrease in the intensity of the XRD lines for t-Se and growth of lines characteristic of α-Se. At the same time, the diffuse background of a-Se reappears, as shown in Fig. 1. Increasing the milling time results in a substantial depression in the amount of t-Se and a significant increase in that of a-Se. After 300 min of milling, the sample is almost fully amorphized with only traces of t- and α-Se. When $t_m \geq 600$ min, a fully amorphous Se sample is obtained, which was also verified by TEM that a uniform amorphous morphology was observed with diffuse rings in the electron diffraction patterns. These results indicated that ball milling of nanocrystalline t-Se induces a phase transformation from t-Se to a mixture of a-Se and α-Se, and eventually into a single a-Se phase. Our results also indicated that further milling of the as-milled a-Se sample (from 600 to 4800 min) does not induce any further reaction. This conclusion has been verified by subsequent DSC measurements.

Figure 2 presents DSC curves at a heating rate of 20 K/min for the Se samples milled for different times. For the as-quenched sample, the DSC curve exhibits an exothermic peak at T_p = 181 °C with a heat release of ΔH = 63 J/g, corresponding to the crystallization of the as-quenched a-Se to nanocrystalline t-Se. After milling for 0.25 min (the sample is still in the "x-ray" amorphous state), the DSC peak shifts to lower temperatures (T_p = 123 °C) and ΔH is slightly decreased. This is due to a change in the molecular structure in the amorphous Se samples as indicated by the IR and RS measurements [11]. Further milling results in an evident decrease in both the peak temperature and the heat release, as shown in Fig. 2. The observed partial crystallization in the a-Se sample induced by milling is responsible for the decrease in the thermal stability of the residual amorphous phase, as also detected in metallic systems [7,8]. For the sample milled for 30 min with

which XRD and TEM showed a fully crystallized *t*-Se state with nm-sized grains, a rather weak exothermic peak was detected with T_p = 83 °C and ΔH = 2.6 J/g, that may be attributed to a grain growth (and strain release) process of nanocrystalline *t*-Se and/or crystallization of the residual a-Se that has not been transformed during milling. With a further extension of milling, the exothermic peak in DSC curve recovers and becomes more and more evident. Both the peak temperature and the peak area raise with an increase of t_m, and tend to stable values of about 95 °C for T_p and 44 J/g for ΔH when $t_m \geq 300$ min. This observation indicates that an amorphous phase is formed, which agrees with the XRD and TEM results, although its thermal stability differs from that of the as-quenched a-Se.

Nanocrystallization of a-Se during ball milling can be understood in terms of MA process, which induces large localized permanent strain in the amorphous sample, that may activate heterogeneous nucleation of crystalline phase in the amorphous matrix. However, more experimental and theoretical investigations are need to reveal the intrinsic mechanism for the MA-induced nanocrystallization.

No visible difference was detected in the as-milled and the as-quenched a-Se by the XRD and TEM measurements, however, DSC results show that the T_p and ΔH values for the as-milled fully-amorphized Se ($t_m \geq 600$ min) are smaller than those for the as-quenched a-Se. Such differences might be attributed to different microstructures of the two types of *a*-Se phase, as revealed by Raman and infrared spectra measurements [11]. Figure 3 shows the Raman spectra for the as-quenched a-Se and the Se samples milled for different periods of time. Quantitative analyses of the characteristic bands exhibiting in different Se samples indicate that the as-quenched *a*-Se is composed predominantly of Se_8 ring molecules and a small fraction of $[Se-]_n$ polymeric chains, while for the as-milled *a*-Se specimen, $[Se-]_n$ polymeric chains were predominant, as in the crystalline t-Se. The result implies that a mixture of Se_8 rings and $[Se-]_n$ chains exhibits a higher thermal stability against crystallization upon heating than the $[Se-]_n$ chains only. Although a fundamental difference in the molecular structure was found in the as-quenched and the as-milled a-Se, x-ray photoemission measurements indicated that no detectable change in electronic properties (e.g. the density of valence states, the binding energies of core levels, and the characteristic energy loss functions) were observed among different states of Se samples [11].

MA induced amorphization mechanism. One of the most striking features observed in our experiments is the fully amorphization of crystalline Se during ball milling. In order to understand the underlying mechanism for solid state amorphization in the pure element, we performed a detailed measurement of the amorphization process with a starting material of coarse-grained crystalline t-Se for ball milling. Figure 4 summarizes the measurement results for the milling process of crystalline Se. It is seen that at the early stage of milling (t_m <30 min, stage I in Fig. 4), the mean grain size of Se (determined by means of XRD) decreases rapidly, while the microstrain (from XRD measurements) goes up. When t_m= 30 min, the grain size decreases down to about 16 nm, but the microstrain reaches a maximum value of about 0.4%, and it drops down with an extension of milling time. By means of XRD analysis of the integrated intensity of the Bragg reflection and the background and the DSC quantitative measurement of the enthalpy change, one noticed that the amorphization process onsets at t_m= 30 min (as seen in Fig. 4b). Determination of the lattice parameters for the nanocrystalline Se indicated that the unit cell volume also shows a jump up by about 0.3% at 30 min (Fig. 4c). In the second stage of milling (as indicated in Fig. 4), the grain size of Se keeps a stable value of about 13 nm, the microstrain gradually decreases, and the lattice distortion value maintains a constant value of about 0.3%. The volume fraction of the amorphous Se increases continuously up to 90% when milled for 120 min. Further milling up to 250 min led to a complete amorphization in stage III, the unit cell volume drops close to the equilibrium value and the grain size decreases to about 9 nm at 200 min. We have not observed *α*-Se phase formation prior to the onset of amorphization, as in the case in Fig. 1. This might be originated from difference in the starting materials (the as-milled t-Se and the annealed crystalline t-Se).

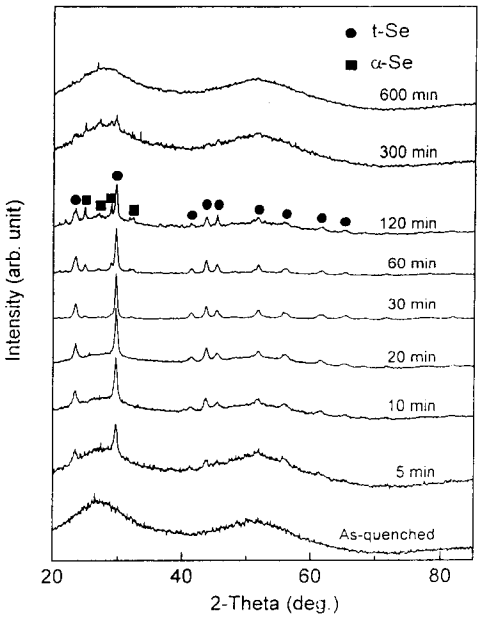

Figure 1 XRD patterns for as-quenched a-Se and the samples milled for different periods of time as indicated.

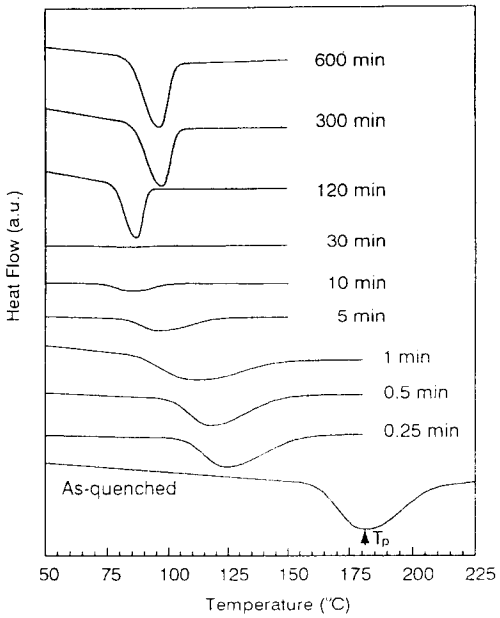

Figure 2 DSC curves at a heating rate of 20 K/min for as-quenched a-Se and the milled Se specimens.

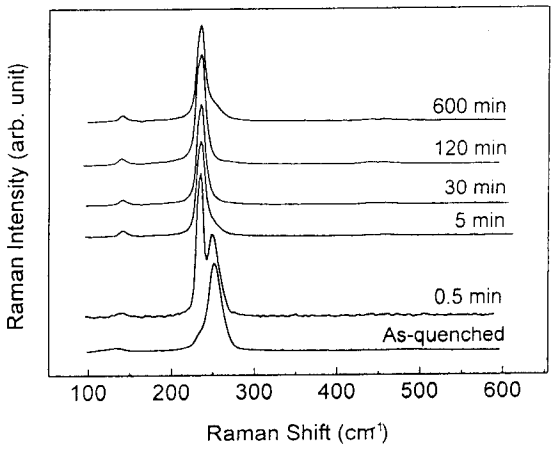

Figure 3 Raman spectra for the as-quenched a-Se and the Se samples milled for different periods of time as indicated.

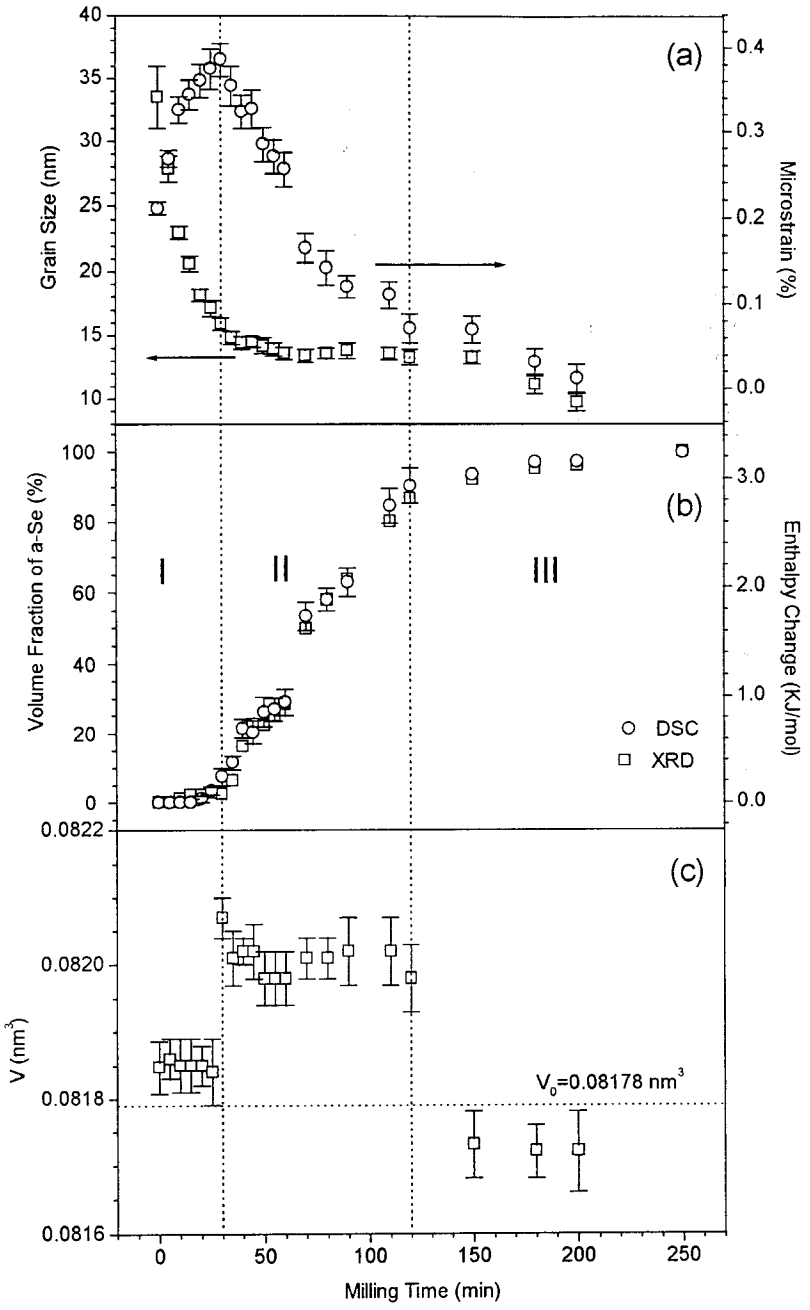

Figure 4 Variation of various structure parameters with the milling time during ball milling of crystalline t-Se: (a) grain size and microstrain, (b) volume fraction of amorphous Se determined from DSC and XRD, and (c) unit cell volume of t-Se lattice.

These observations indicated that amorphization of crystalline t-Se starts when its average grain size is reduced to a certain value (~ 16 nm). This value coincidences with the critical grain size (15.6 nm) estimated from the thermodynamic analysis with which the Gibbs free energies of the nanocrystalline Se and the a-Se phase are equal [12]. During the major amorphization process (5 to 90% volume fraction, stage II), the crystallite size keeps unchanged at about 13 nm. This phenomenon can not be explained following the "skin" model that the amorphous phase nucleated at intercrystallite boundaries and grew into the crystallites by gradually consuming the crystalline phase, resulting in a shrinking of remaining crystallite size. The observed constant grain size during amorphization process implies that the crystallites smaller than a certain grain size (say 13 nm) may be transferred into amorphous completely while those larger than 13 nm keep to be crystalline.

The onset of amorphization corresponds to a drop in the microstrain, indicating the microstrain between the nanocrystallites is relaxed when the amorphous phase is formed. If a layer of amorphous phase is formed along the crystallite boundaries, as described by the "skin" model, the microstrain would diminish when the volume fraction of the amorphous phase reaches a certain value (about 40% with a crystallite size of 13 nm and an amorphous layer thickness of 1 nm), i.e. when all the boundaries are occupied by the amorphous phase. However, our experimental measurements showed that when the amorphization reaches about 90% volume fraction, a substantial microstrain of about 0.1% was detected, meaning the "skin" model is not valid in this case.

The major amorphization process corresponds to an evident lattice distortion of about 0.3% in the nanocrystalline Se, which may contribute to the driving force for the amorphization process. As the measured lattice distortion by means of XRD is an average value over all nanocrystallites, the smaller crystallites may exhibit stronger lattice distortion due to the grain size effect. It has been observed that, in nc Se samples crystallized thermally from the amorphous solid, the lattice distortion increases significantly with a reduction of grain size. A lattice expansion up to 0.7% was detected when the grain size is 13 nm [13,14]. This implies the driving force contribution from the lattice distortion might be significant for the amorphization process in the small crystallites below the critical grain size.

Acknowledgments: This work was financially supported by the Chinese Academy of Sciences and the National Science Foundation of China (Grants No. 59625101 and 59431021).

References

[1] W.L. Johnson: Prog. Mater. Sci. Vol. 30 (1986) 81.
[2] K. Lu: Mater. Sci. Eng. R Vol. R16 (1996) 161.
[3] J. S. C. Jang and C.C. Koch: J. Mater. Res. Vol. 5 (1990) 498.
[4] G.F. Zhou and H. Bakker:Phys. Rev. Vol. B49 (1994) 12507.
[5] T.D. Shen, C.C. Koch, T.L. McCormick, R.J. Nemanich, J.Y. Huang and J.G. Huang: J. Mater. Res. Vol. 10 (1995) 139.
[6] E. Gaffet, F. Faudot and M. Harmelin: Mater. Sci. Eng. Vol. A149 (1991) 85.
[7] M.L. Trudeau, R. Schulz, D. Dussault and A. Van Neste: Phys. Rev. Lett. Vol. 64 (1990)
[8] F.Q. Guo and K. Lu: Metall. Mater. Trans. A Vol. 28A (1997) 1123.
[9] F.Q. Guo and K. Lu: Phil. Mag. Lett. Vol. 77 (1998) 181.
[10] H.Y. Zhang, Z.Q. Hu and K. Lu: Nanostructured Mater. Vol. 5 (1995) 41.
[11] F.Q. Guo and K. Lu: Phys. Rev. B Vol. 57 (1998) 10414.
[12] Y.H. Zhao, Z.H. Jin and K. Lu: to be published.
[13] Y.H. Zhao, K. Zhang and K. Lu: Phys. Rev. B Vol. 56 (1997) 14322.
[14] Y.H. Zhao and K. Lu: Phys. Rev. B Vol. 56 (1997) 14330.

Metastable, Mechanically Alloyed and Nanocrystalline Materials 1998
10.4028/www.scientific.net/MSF.312-314

Mechanically-Driven Solid State Amorphization and Nanocrystallization in Selenium
10.4028/www.scientific.net/MSF.312-314.43